

High-resolution CH stretch spectroscopy of jet-cooled cyclopentyl radical: First insights into equilibrium structure, out-of-plane puckering, and IVR dynamics

Cite as: J. Chem. Phys. 157, 034302 (2022); doi: 10.1063/5.0096946

Submitted: 23 April 2022 • Accepted: 23 June 2022 •

Published Online: 15 July 2022



View Online



Export Citation



CrossMark

Andrew Kortyna,^{1,2}  Melanie A. R. Reber,³  and David J. Nesbitt^{1,4,5,a)} 

AFFILIATIONS

¹JILA, National Institute of Standards and Technology and University of Colorado, Boulder, Colorado 80309, USA

²ColdQuanta, Inc., 3030 Sterling Circle, Boulder, Colorado 80301, USA

³Department of Chemistry, University of Georgia, Athens, Georgia 30602, USA

⁴Department of Chemistry, University of Colorado, Boulder, Colorado 80309, USA

⁵Department of Physics, University of Colorado, Boulder, Colorado 80309, USA

^{a)}Author to whom correspondence should be addressed: djn@jila.colorado.edu

ABSTRACT

First, high-resolution sub-Doppler infrared spectroscopic results for cyclopentyl radical (C_5H_9) are reported on the α -CH stretch fundamental with suppression of spectral congestion achieved by adiabatic cooling to $T_{rot} \approx 19(4)$ K in a slit jet expansion. Surprisingly, cyclopentyl radical exhibits a rotationally assignable infrared spectrum, despite $3N - 6 = 36$ vibrational modes and an upper vibrational state density ($\rho \approx 40\text{--}90 \text{ \#/cm}^{-1}$) in the critical regime ($\rho \approx 100 \text{ \#/cm}^{-1}$) necessary for onset of intramolecular vibrational relaxation (IVR) dynamics. Such high-resolution data for cyclopentyl radical permit detailed fits to a rigid-rotor asymmetric top Hamiltonian, initial structural information for ground and vibrationally excited states, and opportunities for detailed comparison with theoretical predictions. Specifically, high level *ab initio* calculations at the coupled-cluster singles, doubles, and perturbative triples (CCSD(T))/ANO0, 1 level are used to calculate an out-of-plane bending potential, which reveals a C_2 symmetry double minimum 1D energy surface over a C_{2v} transition state. The inversion barrier [$V_{barrier} \approx 3.7(1)$ kcal/mol] is much larger than the effective moment of inertia for out-of-plane bending, resulting in localization of the cyclopentyl wavefunction near its C_2 symmetry equilibrium geometry and tunneling splittings for the ground state too small (<1 MHz) to be resolved under sub-Doppler slit jet conditions. The persistence of fully resolved high-resolution infrared spectroscopy for such large cyclic polyatomic radicals at high vibrational state densities suggests a “deceleration” of IVR for a cycloalkane ring topology, much as low frequency torsion/methyl rotation degrees of freedom have demonstrated a corresponding “acceleration” of IVR processes in linear hydrocarbons.

Published by AIP Publishing. <https://doi.org/10.1063/5.0096946>

I. INTRODUCTION

Intramolecular vibrational energy redistribution (IVR) is expected to impact the rovibrational spectra of large molecules when the density of states enters the $\approx 10^2 \text{ states/cm}^{-1}$ range.¹ As a molecule increases in size and complexity, interaction with the near resonant background states leads to additional splittings and line broadening until high-resolution rovibrationally resolved

spectroscopy becomes impossible. For example, previous jet-cooled spectroscopic efforts^{1–3} revealed significant spectral fragmentation for ν_1 acetylenic C–H stretch excitation near 3300 cm^{-1} in substituted acetylenes (RCCH; R = CH_3 , C_2H_5 , C_3H_8), even though such terminal acetylenes represent relatively small C_4 – C_6 hydrocarbons with a stiff CC triple bond mechanically isolating the CH stretch fundamental from the methyl, ethyl, and propyl groups as much larger sources of vibrational state density. This perspective

was significantly amplified in spectroscopic work by Perry and co-workers^{4–6} on hydrocarbon species with torsional degrees of freedom, which specifically identified low frequency torsional modes accelerating the onset of IVR spectral fragmentation. In fact, the above studies develop a theme initially explored in pioneering studies by Parmenter^{7–9} and Hopkins and co-workers^{10–12} for which the presence of a single methyl group or hydrocarbon tail on an aromatic ring was found to be responsible for a profound IVR induced loss of resolved vibronic spectral structure in the dispersed fluorescence from the electronically excited state.

Indeed, infrared absorption spectroscopy by McIlroy and Nesbitt¹³ of slit jet-cooled 1-butene and *trans*-2-butene made this transition from discrete to continuous absorption explicit, with the *trans*-2-butene species displaying fully resolved albeit spectrally fragmented rovibrational structure, whereas the 1-butene spectra revealed *continuous absorption profiles* even under high-resolution sub-Doppler ($\Delta\nu \approx 40$ MHz) conditions in a cold (20 K) slit jet expansion.^{1,13} This could not be explained simply by differences in vibrational state densities^{14,15} for 1-butene ($\rho \approx 170$ #/cm⁻¹) vs *trans*-2-butene ($\rho \approx 215$ #/cm⁻¹) at the CH stretch excitation energies but, instead, was attributed to low frequency, highly nonharmonic, large amplitude internal rotation of C–C–C torsional coordinate in 1-butene as an “accelerator” for intramolecular vibrational relaxation coupling. Such extreme IVR coupling of CH ($v = 1 \leftarrow 0$) excitation with near resonant background vibrations, thus, reflects a dynamically intriguing limit where high-resolution infrared spectroscopy simply fails, in essence due to strong mixing of the optically accessible “bright” state with the dense manifold of optically inaccessible “dark” states. As this coupling also results in an extreme dilution of oscillator strength from a single “bright” state into a dense manifold of “dark” states, this transition is also accompanied by a comparable loss of sensitivity. Although such a transition from well-resolved/high information content spectra to a limit of near continuous spectral absorption (which a high-resolution spectroscopist might dub “the IVR catastrophe”) must occur eventually, there is still little information on the evolution of such intramolecular vibrational dynamics of molecules throughout this transition region. Indeed, it is not a question of if but, in fact, how high-resolution spectroscopic methods fail as a function of molecular size, the nature of the vibrational mode excited, and density/character of background states that is interesting and will require further exploration.

With the greatly increased path length, number density, and sensitivity for absorption spectroscopy in a slit discharge expansion, this question of the dynamical role of IVR coupling can be extended to open shell systems. Toward this end, we have now successfully explored over a dozen jet-cooled hydrocarbon radicals with high-resolution infrared spectroscopic methods, which for small hydrocarbon species (C₁–C₄) with sufficiently low vibrational state densities all reveal completely resolved and assignable rovibrational structure in the slit jet expansion condition. Indeed, pushing steadily further toward this IVR catastrophe limit, we have previously observed and assigned rotationally resolved C–H spectra of both phenyl^{16,17} (C₆) and benzyl (C₇) radicals.¹⁸ The latter species, in particular, has 14 atoms and $3N - 6 = 36$ vibrational modes, but due to resonance stabilization of the CH₂ radical with the aromatic ring, it exhibits a vibrational/geometric structure that significantly stiffens the ring and methylene group vibrations. Hence, one might argue

that, due to this stiffening ring and methylenic vibrations, the density of states for benzyl radical in the CH stretch region is reduced below some critical level required to facilitate IVR coupling with optically inaccessible (“dark”) resonant bath states and consequent loss of spectral structure.

Cyclopentyl (C₅H₉) radical represents an interesting intermediate case, as it is as large as benzyl radical (14 atoms) yet still a saturated molecule, i.e., with no double bonds or resonance delocalization to stiffen its vibrational structure. One might, therefore, expect such an alkyl radical species to present a significantly large density in the C–H stretch region of its spectrum and, therefore, have a greater potential for loss of rotationally resolved spectrum by “spectral dilution” of the “bright” state oscillator strength. More quantitatively, we can obtain a set of anharmonic vibrational frequencies for cyclopentyl with high level coupled-cluster, singles, doubles, and perturbative triples CCSD(T)/ANO1 calculations, which with the exact state count backtracking algorithms of Kemper *et al.*¹⁹ predict a state density of ≈ 40 –90 states/cm⁻¹ in the C–H stretch region near 3070 cm⁻¹. As a result, cyclopentyl radical state densities lie near the center of the region where one might expect IVR effects to emerge and eventually predominate. Interestingly, however, the spectroscopic results herein reveal that this is in fact not the case. Instead, cyclopentyl radical exhibits rich, well-resolved, and completely assignable high-resolution rovibrational structure in the α -C–H stretch region, with evidence of only relatively modest spectroscopic perturbations in the upper state.

Beyond interest in the elucidation of IVR dynamics, cyclopentyl radical plays an important role in both combustion and atmospheric chemistry. Heavy oil deposits are known to be rich in cycloalkanes,^{20,21} the initial oxidation steps of which are believed to proceed via H atom abstraction radical formation.²² In a climate change-sensitive era where the concentration of atmospheric carbon (predominantly CO₂ and CH₄) is of paramount concern, a more complete understanding of the chemistry, reaction mechanisms, and theoretical benchmarking of these fossil fuels will be required until environmentally green alternative energies are readily available. Unfortunately, the current state of this understanding is quite limited, with very little known about the spectroscopy and structure of such cycloalkyl radical intermediates. What is known comes from spectroscopic studies of the related alkyl peroxy radicals (RO₂·), which are important atmospheric intermediaries in polluted urban environments where reactions with NO and NO₂ contribute to ozone buildup.²³ In environments with low NO_x concentrations, reactions with HO₂ take on special importance. The RO₂· + HO₂ is often modeled assuming R = methyl, but when cyclopentyl is substituted for the radical, it has been found that rate constants are threefold larger and the negative temperature dependence is steeper.²⁴ As is the case for combustion, a better fundamental understanding of cycloalkyl radicals should contribute to similar benefits for atmospheric science.

The structure of closed shell cyclopentane has been extensively studied. For example, infrared (IR) and Raman spectroscopy have shown that there are two conformers of cyclopentane, a twisted C₂ form and a bent C_s form, with nearly identical energies.²⁵ Cyclopentane has also attracted interest for its ability to sustain pseudorotations (for example, see the highly cited articles by Durig and Wertz²⁶ and Bauman and Laane²⁷). In contrast, little has been published on the structure of corresponding open shell cyclopentyl radical

species. The structure of peroxy-cyclopentyl radical (C_5H_9OO), which is an important intermediate in the oxidation of cyclopentane, has been studied in the near IR on the $S_1 \leftarrow S_0$ electronic transition by Thomas *et al.* with cavity ringdown spectroscopy.²² Photoelectron spectroscopy has also been used to study low lying electronic state energies, electron affinities, and thermal decomposition pathways for cyclopentyl.²⁸ To the best of our knowledge, however, the present work represents the first report on rotationally resolved spectroscopy of cyclopentyl radical in either the ground or vibrationally excited states.

The equilibrium structure of cyclopentyl radical is predicted to be a near-oblate top with A and B rotational constants within 5% of each other, as shown in Fig. 1 from density functional theory.²⁹ The two views in this figure reveal the equilibrium structure of the ring to be significantly buckled, consistent with C_2 rotational symmetry about the CH bond at the radical site and coincident with the B principal axis. This calculation at the B3LYP/6-311++g(3df, 3pd) level predicts the anharmonic band origin to be 3059.0 cm^{-1} for the highest energy α -CH stretch and in reasonable agreement ($\pm 10\text{ cm}^{-1}$) with measurements reported herein. We have also performed a more sophisticated set of coupled-cluster calculations using Amlof (ANO0, ANO1) and Dunning's correlation-consistent basis sets (cc-pVDZ and cc-pVTZ).³⁰ These calculations assume C_2 symmetry and predict the highest energy vibration to be dominated by CH stretching motion at the sp^2 radical center, with anharmonic band origins computed at 3071.5 and 3070.1 cm^{-1} , respectively, which are now in remarkable agreement ($<1\text{ cm}^{-1}$) with the experimentally observed band origin at $\nu_0 = 3071.2892(7)\text{ cm}^{-1}$.

In the work reported herein, we use narrowband IR radiation to directly excite one quantum of the highest frequency α -CH stretch (marked with the red arrow in Fig. 1), where the cyclopentyl radical is produced in a pulsed supersonic slit discharge. A highly rotationally resolved spectrum is observed with surprisingly little evidence of perturbative influences, despite a high density ($\rho_{\text{vib}} \approx 40\text{--}90\text{ \#/cm}^{-3}$) of near resonant "dark" states. This spectrum is fitted to a Watson rigid-rotor Hamiltonian that generates the ground/vibrationally excited rotational constants (A, B, and C) and vibrational band origin. The results from these least squares fits can be usefully compared with high level *ab initio* calculations, which prove to be

in encouragingly good agreement. The remainder of this paper is organized as follows: After setting the context for these investigations in Sec. I, Sec. II briefly describes the experimental approach for slit jet discharge formation and detection of cyclopentyl radical, which, contrary to expectations based on vibrational state density, exhibit surprisingly clean, high-resolution absorption spectra with little evidence for extensive spectral fragmentation due to IVR. Analysis of these high-resolution spectra via least squares fits to a Watson Hamiltonian is presented in Sec. III, which provides first precision structural data for this cycloalkyl radical as well as predictions for facilitating spectral searches in future microwave studies. This is followed in Sec. IV by a discussion of high level CCSD(T) *ab initio* predictions for out-of-plane puckering of the C_5 ring and Boltzmann analysis of the rotational distributions and total radical densities. We then continue this theme in Sec. V with calculations of the vibrational state densities by efficient exact state counting algorithms and assessment of the impact of IVR...with random matrix analysis. The paper concludes in Sec. VI with a summary of key points and directions for further exploration.

II. EXPERIMENT

The pulsed slit jet discharge IR absorption spectrometer has been detailed previously.^{18,31} Cyclopentyl radicals are generated in a frequency modulated pulsed slit jet discharge, with narrowband, tunable IR radiation produced via frequency difference generation of two visible single-mode lasers. A near shot-noise limited signal is achieved with a combination of phase-sensitive lock-in detection, -30 dB common-mode noise suppression, and gated integration with active background subtraction. Cyclopentyl radical is created by bubbling an inert carrier gas (70% neon, 30% helium) through a room temperature liquid sample (monohalocyclopentane C_5H_9X , $X = \text{Br}$ or I) and delivering the radical precursor/inert gas mixture to the stagnation region of the pulsed slit jet expansion. Bromocyclopentane has a higher vapor pressure (13 mbar at 25°) than iodocyclopentane (8.5 mbar at 25°),³² but the propensity for electron dissociative attachment is greater for iodine [$D_0(\text{C-I}) + \text{EA}(\text{I}) = -82\text{ kJ/mol}$] compared to bromine [$D_0(\text{C-Br}) + \text{EA}(\text{Br}) = -41\text{ kJ/mol}$].³³ As a result, the higher vapor

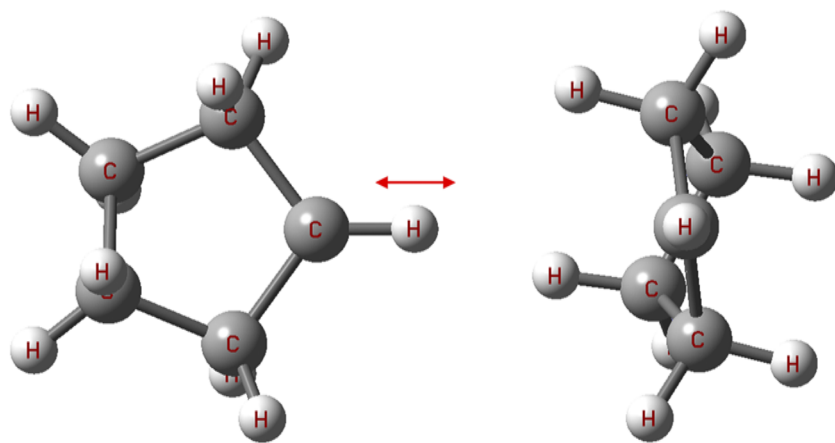


FIG. 1. Near-oblate top structure of the cyclopentyl radical at the density functional level [B3LYP/6-311++g(3df, 3pd)], with arrow (red) displaying the predominant α -CH stretch vibrational motion probed in this study. The right-hand panel view confirms the C_2 symmetry pathway for out-of-plane puckering of the C_5 ring, with a twofold rotational axis coincident with the sp^2 radical α -CH bond.

pressure of the bromine species is roughly balanced by the greater thermodynamic driving force for dissociative attachment of the C-I bond.

For both precursors, the samples are further diluted in He/Ne to 0.5% concentrations and passed at 300 mbar through a $300 \mu\text{m} \times 4 \text{ cm wide} \times 1 \text{ mm deep}$ aperture of a pulsed slit valve. In passage through the 1 mm slit aperture, the mixture enters a region of high electric field (-7.5 kV/cm) in which a discharge is struck, with the discharge field AC modulated at 50 kHz to enable phase-sensitive lock-in detection of transient species. Subsequent expansion into the vacuum chamber of the cyclopentyl radical containing discharge mixture supersonically cools the rotational degrees of freedom down to $T_{\text{rot}} \approx 16(4) \text{ K}$, with essentially all radicals vibrationally cooled into the ground state. This concentrates the initially hot rovibrational partition function for radicals in the discharge environment down into a small number of states with high population density per quantum state. It is this high spatial density per quantum state per volume in the slit jet discharge environment that makes uncongested spectroscopy of such large radical species a feasible prospect.

A periodically poled lithium niobite (PPLN) crystal is used for difference frequency generation between two frequency-stabilized, single-mode lasers: an Ar^+ ion laser at 514.5 nm and a ring dye laser tunable about 610 nm . The resulting IR power is $10\text{--}20 \mu\text{W}$ with an $\sim 1 \text{ MHz}$ linewidth. The tunability of the dye laser allows us to smoothly tune the IR frequency between 3066 and 3075 cm^{-1} needed for this measurement. The frequency of each laser is servo stabilized to independent Fabry-Perot cavities (marker and dye), with the length of the marker cavity locked to an absolute frequency-stabilized HeNe laser.³⁴ The Ar^+ laser frequency is, in turn, also locked to this marker cavity, effectively transferring the long-term ($<1 \text{ MHz}$) stability of the HeNe laser to the Ar^+ laser.³⁴ The ring dye laser scan is then monitored by transmission fringes through the same length-stabilized cavity to which the Ar^+ is locked, thereby providing direct measurement of the infrared difference frequency scan. The frequency reproducibility of the IR absorptions is found be $\pm 11 \text{ MHz}$ ($3.7 \times 10^{-4} \text{ cm}^{-1}$), with the absolute IR frequency scale referenced to four absorption lines in the methane $\nu_3 \text{ R}(4)$ manifold.³⁵ The frequency calibration on these methane lines is 3.3 MHz , which when combined in quadrature with the radical frequency measurement translates into an absolute frequency uncertainty of 12 MHz ($3.8 \times 10^{-4} \text{ cm}^{-1}$).

The absorption signal is monitored with a pair of matched InSb detectors, with the IR beam split into equal powers sent along two paths. One path leads directly to the reference detector, which with fast current mirror subtraction electronics provides -30 dB common-mode reduction in intensity noise cancellation in a 1 MHz servo loop bandwidth. The second IR beam passes into the vacuum chamber containing the radical beam and enters a 16-pass Herriott cell centered on the radical beam a few millimeters beyond the pulsed valve/discharge. The Herriott cell is oriented along the long axis of the slit aperture, providing a total absorption path length of 64 cm . Compression of molecular velocities in the slit expansion axis plus transverse probing parallel to the slit axis suppresses the Doppler width to $\approx 60 \text{ MHz}$, limited by residual non-orthogonal laser crossings of the expansion in a Herriott cell multipass.³⁶ The IR beam exits the vacuum chamber where it encounters a second matched InSb detector, with phase-sensitive detection electronics locked to the 50 kHz modulation of the discharge field. Careful

alignment/focusing onto signal and reference IR detectors, gated integration of the lock-in signal, and active baseline subtraction translates into typical absorbance noise at the $<1 \times 10^{-6}$ absorbance/Hz^{1/2} level, within a factor of three of the “quantum shot-noise” limit due to arrival and detection of individual IR photons.

III. RESULTS AND ANALYSIS

The rotationally resolved absorption spectrum of cyclopentyl is observed and recorded from 3066 to 3075 cm^{-1} , with a moderate resolution representation of the data presented in Fig. 2. To ensure reliability and reproducibility of spectral measurements, each transition in this spectral range is scanned at least three times. Integration times of 16 ms (16 pulses) per frequency element are exploited for the most important spectral region between 3070 and 3073 cm^{-1} , with shorter integration times of 4 ms (4 pulses)/frequency step outside this region. Even at such high visual compression, the strongest P and R branch progressions [$(J \pm 1)_{1,(J \pm 1)} \leftarrow J_{0,J}$ and $(J \pm 1)_{0,(J \pm 1)} \leftarrow J_{1,J}$] are clearly evident (in green), in good agreement with PGOPHER simulations (in red, downward pointing) predicted from the Watson Hamiltonian spectral fits. Traditional asymmetric top notation (i.e., J_{K_a,K_c}) is used throughout, where J is the total angular momentum, and K_c and K_a the approximate projections of J along the corresponding a and c molecule fixed axes. As expected for such a near-oblate top ($A \approx B > C$) molecular radical, the lowest $\Delta K_a = 1 \leftarrow 0$ and $0 \leftarrow 1$ progressions are strongly overlapped and remain unresolved within the residual Doppler widths (60 MHz) in the slit jet expansion. This makes it challenging to unambiguously ascertain the a -vs b -type nature of the rovibrational band, though both band-types provide an approximately equivalent

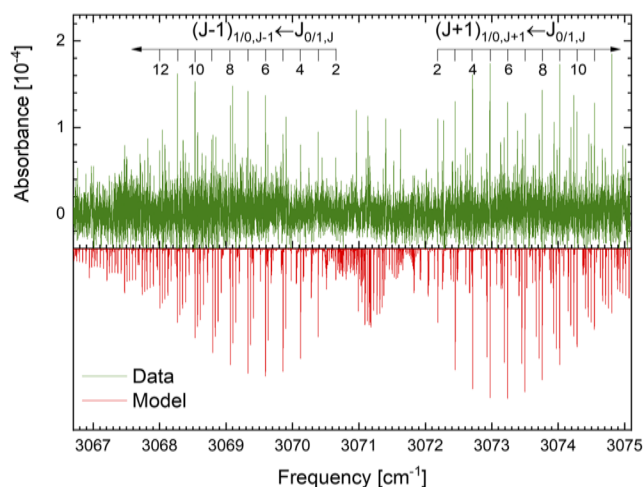


FIG. 2. The α -CH stretch band of cyclopentyl radical. The top (green) trace exhibits a sample scan over the full absorption band under $T_{\text{rot}} \approx 19(4) \text{ K}$ slit jet expansion conditions, with the predominant progression of b -type ($K_a: 1 \leftarrow 0$ and $K_a: 0 \leftarrow 1$) transitions indicated above (black) by railroad tie diagrams. The bottom (red) trace displays model results based on spectroscopic constants obtained from least squares fits of the full spectral data to a rigid-rotor asymmetric top Hamiltonian.

quality of assignment and least squares spectral fit. It is important to clarify that spin rotation splitting for such a large molecular radical is on the sub-60 MHz level and, thus, too small to be resolved even in the slit jet expansion geometry. Thus, in our notation, J really reflects the end-over-end tumbling quantum number normally designated as N .

Figure 3 presents a less visually compressed portion of the spectrum, which displays a sample region in the R branch in higher resolution detail. In addition to demonstrating the excellent success of the spectral simulation, the blue arrows highlight how R branch b-type lines corresponding to a single $J' \leftarrow J''$ manifold are spread out over several spectroscopic groupings, clearly characteristic of the near-oblate asymmetric top behavior expected for cyclopentyl radical. Indeed, a near-oblate top Hamiltonian predicts closer albeit still well-resolved R/P branch $J' \leftarrow J''$ progression for the sequence of $K_a'' + K_c'' = J'', J'' + 1$, as highlighted in red (see Fig. 3) between 3073.9 and 3074.1 cm^{-1} , a pattern reiterated in both R and P branches. Both of these spectral patterns contrast dramatically with the corresponding behavior predicted for a near-prolate top, for which a-type transitions arising from a given $J' \leftarrow J''$ manifold would be very tightly spaced. Finally, once again, unlike spectra for smaller radical species, the expected spin rotation splittings are much less than the sub-Doppler linewidths in the slit jet and, therefore, too small to be resolved.

Spectral analysis is performed using the PGOPHER spectral simulation package,^{37,38} based on least squares fits of the spectral data to a Watson Hamiltonian. From simple bond dipole expectations, this transition moment is predicted to lie along C_2 axis of symmetry (the α -CH bond direction), which exhibits slightly greater perpendicular displacement of H atoms and a larger moment of

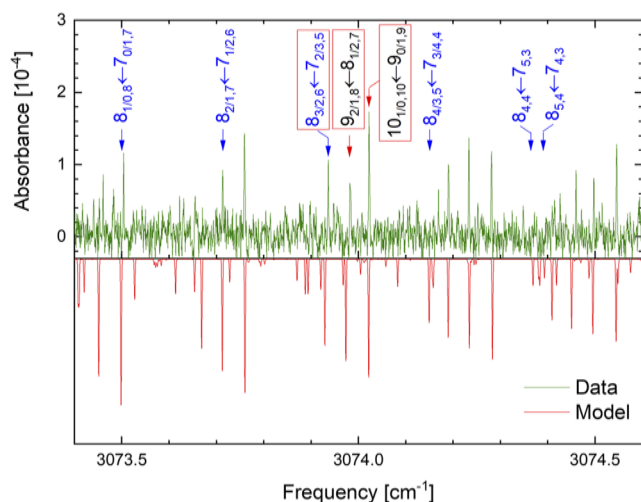


FIG. 3. A high-resolution blowup of the α -CH stretch fundamental R branch region for cyclopentyl radical. The top (green) trace shows the measured absorption band. The blue labels show how the K_a , K_c sublevels in a particular $J' \leftarrow J''$ transition submanifold are spaced out for a near-oblate top spectrum, with the red boxes illustrating the distribution of $J' \leftarrow J''$ transitions within a $\Delta K_a = \pm 1$ grouping. The inverted bottom (red) trace displays PGOPHER simulation results from least squares fits of the full spectrum to a rigid-rotor Hamiltonian.³⁷

TABLE I. Cyclopentyl rovibrational constants for the ground and α -CH vibrationally excited state, with band origin, ν_0 , for the highest energy C–H stretch mode listed on the second line. Units are in cm^{-1} , with uncertainties representing the least significant digit in parentheses. The fit uses a 1r representation and an A reduction to fit a total of 117 observations to an asymmetric top rigid-rotor Hamiltonian with a residual standard deviation of 0.002 cm^{-1} . The third line shows results for a coupled-cluster singles, doubles, and perturbative triples [CCSD(T)] calculation for a frozen core PVnZ ($n = 2, 3$) and ANOn ($n = 0, 1$) basis set in C_2 symmetry. The computed rotational constants are for the ground state and the band origin is from CFOUR anharmonic calculations [CCSD(T)/PVTZ] for the α -CH stretch vibrational fundamental.

Mode	A_v	B_v	C_v	ν_0
Ground	0.2488(5)	0.2358(5)	0.13170(3)	...
α -CH	0.2410(20)	0.2410(20)	0.13162(3)	3071.2892(7)
CCSD(T)	0.234	0.220	0.129	3070.1

inertia and, therefore, represents the B principal rotational axis. As noted above, however, the highly overlapping nature of near-oblate symmetric top transitions for cyclopentyl radical makes it difficult to differentiate between a-type and b-type bands. We handle this by constructing a-type and b-type lists of transition assignments and then fitting a rigid-rotor Hamiltonian to both sets of data. Such an approach reveals the b-type band fits to be marginally superior over those assuming an a-type band, which is also in agreement with physical expectations based on H atom mass distribution in cyclopentyl radical and alignment of the C_2 and B principal axes. We succeed in assigning 59 and 58 b-type transitions in the P and R branches, respectively, (see the [supplementary material](#) for a list of assignments). Fits of these 117 assigned transitions to a rigid asymmetric top Watson Hamiltonian yields A, B, and C rotational constants for the vibrationally ground and the excited states and the band origin for the vibrationally excited state. The fit results are summarized in Table I, along with predictions from high level [CCSD(T)/PVTZ] calculations using the CFOUR *ab initio* quantum chemistry code platform.³⁰ Immediately worth noting are the lower state rotational constants, which demonstrate a near planar behavior ($A \approx B \approx 2C$), yet also with quantitative spectroscopic evidence for deviations from a perfect oblate top in Ray's asymmetry parameter [$\kappa = (2B - A - C)/(A - C) \approx 0.778(5)$]. Such behavior is in good agreement with equilibrium predictions of κ from CFOUR ($\kappa_{\text{eq}} \approx 0.727$) and indicative of a strong C_2 symmetry deformation of the C_5 ring away from planarity.

IV. DISCUSSION

A. Comparison with *ab initio* calculations

The near-oblate yet asymmetric top nature of cyclopentyl is borne out by the measured rotational constants reported in Table I. For the ground state, the measured A and B rotational constants differ significantly (by 18σ) but with A and B comparable in size ($<5\%$) and the C constant approximately twofold smaller ($A \approx B \approx 2C$), as characteristic for a predominantly planar molecular geometry. This is consistent with our highest level coupled-cluster calculations in Table I [CCSD(T)/PVTZ] with A and B varying by 6% and C, again, about a factor of two smaller. Interestingly, this non-oblateness decreases significantly

for the upper α -CH stretch vibrationally excited state, with the measured A and B constants now indistinguishable at our level of fitting precision. It is worth noting that the *ab initio* values are systematically lower than those observed experimentally, consistent with a slight (few %) overestimation of the CC bond lengths.

Determining the exact nature of the vibrational motion being observed is not always straightforward for a molecule with 36 vibrational modes, especially with the nine highest energy modes as CH stretches. We can, however, be confident of the “bright” CH stretch character of the vibrational motion being probed because the vibrational band origin is situated well within the C–H spectral region displayed by myriad alkyl molecules. Our analysis of the transition band as *b*-type indicates that the *b* principal rotation axis is parallel to the transition dipole moment. The *c* principal axis (with the largest moment of inertia) is certainly perpendicular to the C_5 ring. The fact that C shrinks slightly ($\approx -0.1\%$) with vibrational excitation further supports the notion that the anharmonic CH stretch vibrational motion is predominantly perpendicular to the *c* axis.

For more unambiguous confirmation of the vibrational motion under study, we turn to quantum chemistry electronic structure calculations.³⁰ Both sets of calculations predict the highest energy vibrational mode to arise from CH displacement along the α -CH bond at the radical center (see the arrow in Fig. 1). Specifically, density functional calculations [B3LYP/6-311++g(3df, 3pd)] estimate the α -CH anharmonic band origin at $\nu_0 = 3059.0 \text{ cm}^{-1}$ (i.e., 11 cm^{-1} too low), with higher level anharmonic coupled-cluster calculations [CCSD(T)/PVDZ, PVTZ] both predicting a band origin within 1 cm^{-1} of the measured value. All three sets of calculations predict the next lower vibrational modes as closely spaced symmetric and antisymmetric stretching of H atoms covalently bound to sp^3 hybridized β -C atoms in the ring, for which one anticipates anharmonic band origins $\approx 100 \text{ cm}^{-1}$ lower in energy, i.e., far enough to be ruled out as contender for the vibrational band observed. In simple freshman chemistry terms, halogen removal results in sp^2 hybridization of the C radical center, and, thus, a stiffer mode and higher vibrational frequency for the corresponding α -CH bond.

B. Boltzmann analysis

It is of interest to characterize the concentration and rotational distributions of cyclopentyl radicals generated in the slit expansion source, which requires normalizing the measured transitions to Hönl–London line strengths, M_J degeneracy, and knowledge of nuclear spin statistical weights due to four pairs of identical spin $1/2$ H atoms (for $2^8 = 256$ spin states) present in cyclopentyl radical that are exchanged over a feasible barrier.^{39,40} From symmetry, one can readily predict a 136:120 = 1.13:1 ortho:para nuclear spin ratio for $K_a + K_c = \text{odd:even}$. Figure 4 shows the results of such a Boltzmann analysis, i.e., a semi-log plot of integrated transition intensities S scaled to quantum degeneracies (both $M_J = 2J + 1$ and $g_{\text{ortho}} = 136/g_{\text{para}} = 120$ nuclear spins) and Hönl–London factors vs ground state rotational energy $E_{\text{rot}}(\nu'', J'')$. If we take all these factors together and assume complete thermal rotational equilibrium, the expected relationship between these integrated line strengths and rotational state populations is simply

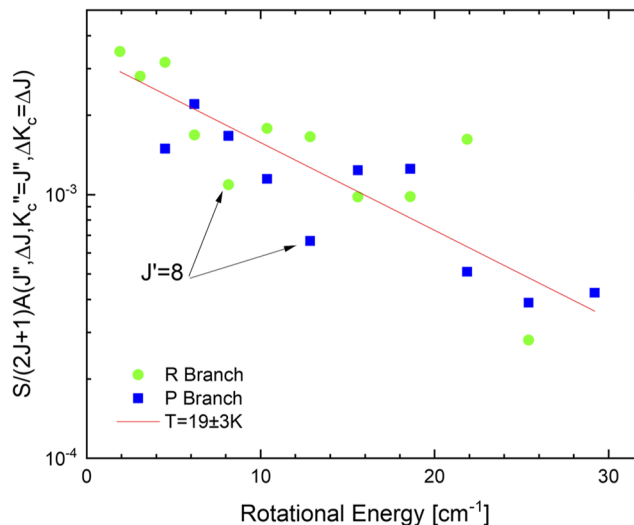


FIG. 4. Boltzmann analysis of cyclopentyl radical for the $K_a: 1 \leftarrow 0$ and $K_a: 0 \leftarrow 1$ *b*-type progressions, with the vertical axis reflecting the integrated absorbance of each spectroscopic peak scaled by nuclear spin statistics, rotational degeneracies, and Hönl–London factors. An exponential fit provides a rotational temperature of $19 \pm 3 \text{ K}$, with the two transitions to the $J' = 8$ vibrationally excited state indicated. The large frequency residuals ($+0.006 \text{ cm}^{-1}$) in the least squares fits and suppression of P and R branch transition intensities provide confirming evidence for a local rotational crossing in the vibrationally excited $\delta_{0,1,8}$ state.

$$S_{ij} = S_0 \times l \times (2J + 1)A(J', J)g_{\text{NS}}[\text{cyclopentyl}]_{\text{tot}} e^{-\frac{E_{\text{rot}}(\nu'', J'')}{kT}} / Q(T), \quad (1)$$

where S_{ij} is the measured integrated line intensity (typically in absorbance $\times \text{MHz}$) for a given $i \leftarrow j$ transition, S_0 the total integrated band intensity ($\text{cm}^2/\text{molecule} \times \text{MHz}$), l the slit path length, $A(J', J)$ the Hönl–London factor, g_{NS} the nuclear spin degeneracies, $[\text{cyclopentyl}]_{\text{tot}}$ the total density of cyclopentyl radicals ($\#/\text{cm}^3$), and $Q(T)$ the rotational partition function. The resulting semilogarithmic plot of $S_{ij}/[(2J + 1)A(J', J)g_{\text{NS}}]$ vs lower state E_{rot} is presented in Fig. 4, for which a linear least squares fit yields a rotational temperature of $19 \pm 3 \text{ K}$. Of equal importance from Eq. (1), the intercept of the Boltzmann plot contains valuable quantitative information on total radical concentration per quantum state $[\text{cyclopentyl}]_{\text{tot}}/Q(T)$ in the slit discharge, which with knowledge of the absorption path length ($l = 64 \text{ cm}$) and *ab initio* integrated absorption strength ($S_0 = 20.31 \text{ km/mol}$)²⁹ can be accurately estimated to be $[\text{cyclopentyl}]_{\text{tot}}/Q(T) \approx 9.3 \times 10^8 \#/\text{cm}^3$. We could in principle also do this by visual comparison with PGOPHER simulations, but the least squares fit method provides more reliable results. If we therefore extrapolate back to the slit expansion orifice based on a $1/r$ drop-off in density, this predicts $[\text{cyclopentyl}] \approx 1.0 \times 10^{13} \#/\text{cm}^3$, which can be usefully compared with an average precursor density in the middle of the 1 mm slit discharge of $\approx 0.75 \text{ Torr} = 2.4 \times 10^{16} \#/\text{cm}^3$. Thus, although $10^{13} \#/\text{cm}^3$ represents a reasonably high radical density, it reflects only a modest efficiency ($\approx 0.042\%$) for dissociative attachment of halocyclobutane precursor by low energy electrons, limited by $\approx 10^5 \text{ cm/s}$ supersonic expansion

speeds and, thus, the short time ($\approx 1 \mu\text{s}$) spent in the discharge environment.

Due to a high abundance of low energy $J_{K_a K_c}$ levels and, thus, high density of spectral transitions for an oblate top at low rotational temperatures, the signal-to-noise ratio is limited ($S/N = 10:1$), even for the long path lengths and relatively high densities of radicals in the slit jet discharge expansion. As a result, the familiar pattern of uniform spacings in P/R branches contributes to additional ambiguity in the J assignment. One interesting feature worth noting in this regard from Fig. 2 is the presence of the small but clear dips in intensity evident for the pair of P/R branch transitions accessing the same upper $8_{0/1,8}$ levels, which for such a near-oblate top remain unresolved even at our spectral resolution. This plus a matching blue shift in the corresponding P/R branch transition pair provides unambiguous evidence for a localized rotational crossing and, therefore, weak perturbative mixing of these upper state $8_{0/1,8}$ levels with near resonant “dark” states in the excited vibrational manifold. Given that the total harmonic/anharmonic vibrational density of states for cyclopentyl radical at 3070 cm^{-1} is $\sim 40\text{--}90 \text{ states/cm}^{-1}$, the presence of such an isolated rotational crossing is not surprising. Indeed, it is the lack of evidence for many more such “perturbations” that is more remarkable, a point to which we will return in Sec. V. For the moment, however, the spectral and intensity evidence for this isolated rotational crossing offers one valuable side benefit, specifically confirmation of the correct J state assignment progression, which unambiguously identifies pairs of P/R branch transitions ($8_{1/0,8} \leftarrow 7_{0/1,7}$ and $8_{1/0,8} \leftarrow 6_{0/1,6}$) to the same upper state. Additional evidence supporting this hypothesis is also found in the Watson Hamiltonian spectral analysis, for which the $8_{1/0,8} \leftarrow 7_{0/1,7}$ and the $8_{1/0,8} \leftarrow 6_{0/1,6}$ transitions have symmetric fitting residuals ($+0.006 \text{ cm}^{-1}$) threefold greater than the average rms residuals ($\pm 0.002 \text{ cm}^{-1}$) for the overall least squares fit.

C. 1D potential energy surface for out-of-plane puckering

The availability of high-resolution infrared spectroscopic data for gas phase cyclopentyl offers important first insights into the geometric structure and unimolecular dynamics of five-membered ring radicals. First of all, the nearly oblate yet still significantly asymmetric top nature of the rotational constants ($\kappa = 0.757$) makes clear that there must be considerable puckering of the C_5 ring. We have explored this by high level *ab initio* [CCSD(T)/ANOn, $n = 0, 1$] calculations, which confirm the existence of two equivalent ground state equilibrium structures connected over a C_{2v} transition state ($\omega = 1751 \text{ cm}^{-1}$, see Fig. 5) via C_2 symmetry vibrational displacement of the coordinates. The C_{2v} barrier height (3.7 kcal/mol) is well converged, with values at the PVTZ, ANO0, and ANO1 levels differing by only 0.1 kcal/mol. Vibrational calculations indicate this to be a second order transition state, with an additional low frequency imaginary vibration ($\omega = 55i \text{ cm}^{-1}$) leading to a second higher local minimum in C_5 symmetry, which then can further distort upon C_2 displacement to the ground state C_2 global minimum.

The presence of a clear double minimum (see Fig. 5) in the C_2 puckering coordinate makes an unambiguous prediction for tunneling dynamics in the vibrational ground state, which if

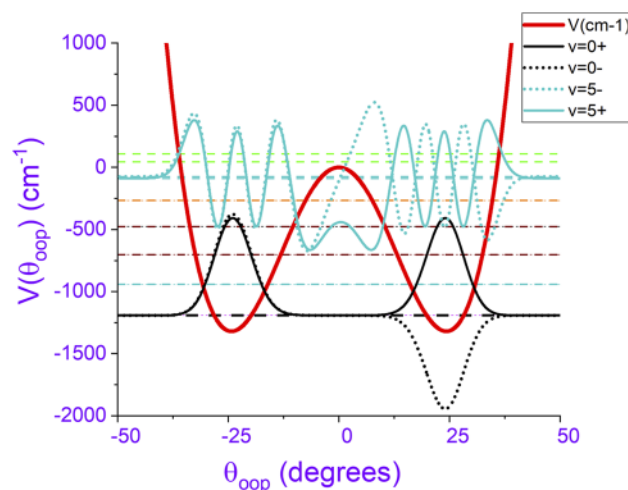


FIG. 5. Out-of-plane puckering potential energy surface for cyclopentyl radical, calculated along a relaxed C_2 symmetry path at the CCSD(T)/ANO0 level. The calculations indicate the clear presence of a significant barrier [$E_{\text{barrier}} = 3.7(1) \text{ kcal/mol}$, C_{2v} symmetry] at the planar C_5 ring geometry ($\theta_{\text{oop}} = 0^\circ$), which results in a double minimum tunneling potential. In addition, puckering eigenvalues and selected eigenfunction pairs ($v = 0^\pm$, $v = 5^\pm$) for the out-of-plane vibration coordinate are indicated, based on vibrationally adiabatic treatment of large amplitude motion with the lamm.exe utility from Multiwell⁴² followed by Numerov integration of the 1D Schrödinger equation. The tunneling splitting for the lowest pair of levels ($v = 0^\pm$) is predicted to be $< 1 \text{ MHz}$, which is not resolved with current slit jet IR spectrometer but should be detectable via microwave spectroscopy.

measurable would inform on the height of the tunneling barrier. To explore this further, we have analyzed the cyclopentyl geometries along the C_2 transition path using the LAMM software package available in Multiwell,^{41,42} which allows us to extract a moment of inertia $I(\theta_{\text{oop}})$ and effective internal rotational constant $B(\theta_{\text{oop}}) = 2I(\theta_{\text{oop}})/\hbar^2$ as a function of the out-of-plane puckering angle θ_{oop} . We then use the large amplitude methods clearly described by Rush and Wiberg, which, in turn, are based on the impactful Hamiltonian “rigid bender” papers of Hougen, Bunker, and Johns, to calculate and converge eigenvalues and eigenfunctions for this puckering motion.^{43,44} The ground (0^+) and first excited (0^-) tunneling state eigenfunctions are displayed in Fig. 5, with the lowest ten eigenvalues up to the inversion barrier indicated by dashed lines. Of particular importance, the inversion barrier is sufficiently high with respect to $B(\theta_{\text{oop}})$ to quench the ground tunneling splittings to $< 1 \text{ MHz}$ levels, i.e., much smaller than our residual infrared Doppler widths [50(5) MHz] and, thus, not observable in the slit jet expansion. However, these predicted tunneling-rotational splittings should be feasibly detectable in microwave studies (e.g., by McCarthy and co-workers),^{45–47} toward which the availability of first precision rotational constants for gas phase cyclopentyl radical offers suitable guidance and encouragement. Finally, it is worth noting that such splittings in the spectra, if resolved, would in fact reflect differences between tunneling splittings in the lower and upper vibrational states. Hence, the lack of resolution of such splittings in the experimental spectra could in principle arise from a perfect cancellation of lower/upper state splittings or, more probably, the lack

of resolvable tunneling structure in both upper and lower vibrational states.

V. DENSITY OF STATES AND THE ONSET OF IVR

The studies described above demonstrate the success of high-resolution infrared spectroscopic methods for even large polyatomic hydrocarbon species, such as those observed in the α -CH stretch spectrum for cyclopentyl radical. The existence of high-resolution, assignable, and least squares analyzable asymmetric top rovibrational structure in the spectra clearly confirms that the excited states, at least in the highest frequency α -CH manifold, mix only relatively weakly with the high density of background vibrational levels. We do see evidence for an isolated rotational crossing of the bright state manifold with this background state density, but this seems to occur infrequently. This is dramatically different from the behavior observed in species such as 1-butene, where coupling of the “bright” CH stretch fundamental with background “dark” vibrational states is so extensive that the jet-cooled absorption spectrum is essentially continuous, even at $T_{\text{rot}} < 20$ K and with $\Delta\nu \approx 50$ MHz sub-Doppler linewidths. This vibrational stability of α -CH stretch excited cyclopentyl radical is therefore surprising and warrants discussion as to what might make such a large molecule less susceptible to IVR.

We start by using our highest level *ab initio* calculations [CCSD(T)/PVTZ] of vibrational frequencies with explicit “backtrack” state counting algorithms of Kemper and Buck to calculate the density of vibrational states as a function of internal energy.¹⁹ The resulting densities of background states for cyclopentyl radical are displayed in Fig. 6 for three characterizations of the vibrational level pattern in a given mode: (i) purely harmonic, (ii) VPT2 anharmonic (including cubic and quartic terms in the potential), and (iii) direct state count for the out-of-plane puckering mode (see Fig. 5) with the remaining $3N - 7$ modes treated as anharmonic oscillators. The rapid rise in vibrational state density with internal energy (E_{vib}) is evident, with harmonic/anharmonic ($\rho \approx 40\text{--}50$ $\#/cm^{-1}$) and direct state count ($\rho \approx 90$ $\#/cm^{-1}$) predictions well into the critical $\rho \approx 100$ $\#/cm^{-1}$ density range (blue band in Fig. 6) previously identified for onset of strong IVR mixing with the “bright” CH stretch fundamentals.^{1,4,6,13} It is, thus, remarkable that the spectra for jet-cooled cyclopentyl radical remain discrete, high-resolution, and fully assignable within the perspective of a rigid asymmetric top Hamiltonian.

Although further theoretical and experimental efforts will clearly be necessary to settle this matter definitively, we offer the following preliminary thoughts and analysis. One simple speculation is that this behavior is due to the closed ring topology of the cycloalkyl species, which, in turn, influences the efficiency of intramolecular bright/dark state coupling. Such a dynamical scenario could arise from the competition and/or synergism of two effects: (i) a reduction in the background state density at CH stretch excitation energies due to the ring topology or (ii) a systematic decrease in the average off-diagonal coupling matrix elements (V_{ij}) between bright and dark state manifolds. Contributions from the first source have already been explored in Fig. 6, which from direct back tracking counting methods indicate a density of states at typical CH stretch fundamental energies (3070 cm^{-1}) to be on the order of $\rho \approx 40\text{--}90$ $\#/cm^{-1}$ for this C_5 ring species. We can compare

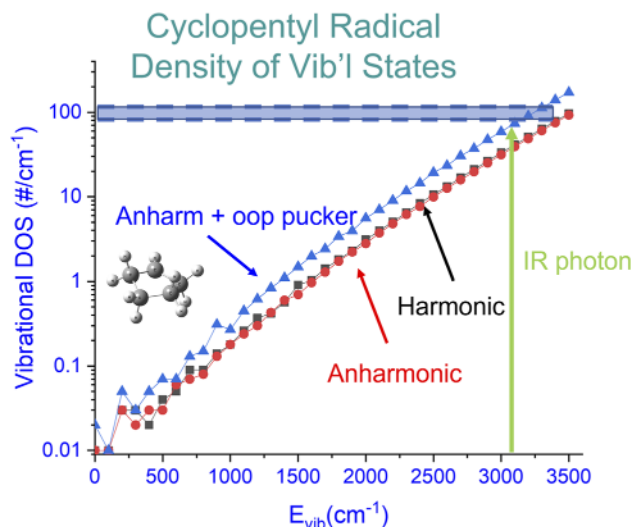


FIG. 6. Vibrational density of states calculated for cyclopropyl radical at the CCSD(T)/PVT2 level with VPT2 anharmonically corrected frequencies. Vibrational states are counted and sorted explicitly into 100 cm^{-1} bins via the efficient back tracking algorithm of Kemper *et al.*¹⁹ The density of states from harmonic (first order), anharmonic (second order) calculations are shown in black (squares) and red (circles), respectively, with the blue symbols (triangles) representing densities based on treating the oop tunneling eigenvalues (see Fig. 5) separately as an explicit anharmonic progression. Note that the predicted cyclopentyl radical densities for α -CH stretch fundamental excitation are $40\text{--}90$ $\#/cm^{-1}$, i.e., in the 100 states/ cm^{-1} range identified for intramolecular vibrational relaxation (IVR) effects to predominate in many simpler closed shell linear hydrocarbon molecules.

this with similar state density predictions of 170 $\#/cm^{-1}$ (1-butene) and 215 $\#/cm^{-1}$ (*trans*-2-butene) for linear C_4 hydrocarbon species, which are clearly significantly higher even for hydrocarbons with one fewer C atom. Such a systematic trend toward a “topological suppression” in state density has also been explored in aromatic C_6 and C_7 ring radical species, for which the relevant symmetry-unsorted state densities at CH stretch fundamental energies are reduced dramatically to $\rho \approx 1$ $\#/cm^{-1}$ and $\rho \approx 67$ $\#/cm^{-1}$ for phenyl (C_6H_5) and benzyl (C_7H_8) radicals, respectively. As this involves only vibrational state counting and no intramolecular relaxation coupling dynamics, this reduction in state density for similar CH stretch energies must clearly arise from the topological elimination of low frequency torsional modes in a linear vs ring hydrocarbon geometry.

We can also explore such effects on the magnitude of the coupling matrix element between bright and dark states. To do this, we recall the systematic blue shifts of $+0.006$ cm^{-1} observed for cyclopentyl spectral transitions accessing the $J' = 8_{08}/8_{18}$ upper states, which signaled shifts due to a local rotational crossing. We can model such shifts from random matrix theory,⁴⁻⁶ where the $(N + 1) \times (N + 1)$ Hamiltonian matrix is constructed in a basis of a single bright state embedded in a bath of N dark states, with matrix elements H_{ij} ($i = 1, j = 2, N + 1$) selected from a simple normal distribution with given mean and rms values. Based on the work of Lawrence and Knight,^{48,49} these N dark states can be treated without approximation as “prediagonalized” with respect to each

other, i.e., with the off-diagonal matrix elements $H_{ij} = 0$ for $i \neq 1$, $i \neq j$ and diagonal matrix elements ($H_{ii} \neq 0$, $i > 1$) chosen from a random distribution representing the local density of dark states, ρ . Diagonalization of these random $N + 1 \times N + 1$ matrices yields a corresponding distribution of eigenvalues and eigenvectors, for which shifts in the bright state and dilution of bright state character can be predicted as function of off-diagonal coupling matrix element distribution. By comparison with the experimentally observed shifts of $\Delta\nu = 0.006 \text{ cm}^{-1}$ for an assumed background density of $\rho \approx 100 \text{ \#/cm}^{-1}$, the average bright–dark state coupling matrix element can be estimated to be $\langle H_{ij} \rangle \approx 0.003(1) \text{ cm}^{-1}$. By way of confirmation, analysis of the eigenvectors also predicts an average 40% dilution of bright state character into the dark state manifold, which is in excellent agreement with the $\approx 40\%$ intensity dips in the P/R branches observed experimentally (see Fig. 2). Finally, the fact that these shifts occur in only a single P/R branch transition pair to $J'_{\text{KaKc}} = 8_{0/1,8}$ is consistent with a rotational crossing between two manifolds with $\Delta(A + B)/2 \sim \langle H_{ij} \rangle/2(J + 1) \approx 1.7 \times 10^{-4} \text{ cm}^{-1}$. Based on the eightfold larger ($1.3 \times 10^{-3} \text{ cm}^{-1}$) shift in $(A + B)/2$ between the ground and vibrationally excited state, this condition is likely to be satisfied. Most importantly, this rms off-diagonal matrix element $\langle H_{ij} \rangle \approx 0.003(1) \text{ cm}^{-1}$ is not exceptional and lies in the middle range of bright–dark state off-diagonal couplings (H_{ij} 0.001–0.007 cm^{-1}) measured from high-resolution infrared spectroscopy for other hydrocarbon molecules.^{1–3,13} Although more work will be necessary, the data suggest that a ring vs linear molecule topology and, therefore, the absence of low frequency torsional modes are primarily responsible for the survival of high-resolution infrared spectroscopy in species as large as cyclopentyl radical.

VI. SUMMARY AND CONCLUSION

Cyclopentyl radical has been detected for the first time via rotationally resolved direct infrared absorption spectroscopy on the α -CH stretch fundamental, with the radicals formed through dissociative electron attachment in a pulsed slit supersonic jet discharge of bromocyclopentane or iodocyclopentane seeded in 70%/30% Ne/He. Phase-sensitive detection of the signal is achieved by modulating the discharge voltage at 50 kHz, with phase-sensitive detection, gated integration, and active background subtraction to reduce noise-levels by ~ 30 dB down to near the quantum shot-noise limit. High-resolution infrared absorption spectra for cyclopentyl radical are obtained for single quantum vibrational excitation in the highest energy α -CH stretch mode on the sp^2 radical C atom.

In light of intramolecular vibrational coupling effects, the large number ($3N - 6 = 36$) of vibrational degrees of freedom in cyclopentyl radical raises the issue of whether a rotationally resolved spectrum can be measured in the CH stretch region. Remarkably, we measure a rich spectrum of discrete, assignable, rotationally resolved transitions indicating that the density of background states ($\rho \approx 40\text{--}90 \text{ states/cm}^{-1}$) is insufficient for extensive bright–dark state mixing due to intramolecular vibrational energy redistribution (IVR). In fact, least squares fits of the spectra to a rigid asymmetric top Hamiltonian are excellent and provide first structural information on this important radical species, which indicate it to be strongly

puckered and yet offer precision predictions with which to facilitate future microwave studies.

To aid in the assignment and interpretation of the spectra, *ab initio* calculations have been performed at both the density functional and more sophisticated coupled-cluster [CCSD(T)] level. In particular, anharmonic CCSD(T)/PVTZ/VPT2 calculations predict the experimentally observed vibrational band origin to within 1 cm^{-1} . We follow this up with high level CCSD(T)/ANO0/1 grid calculations for a C_2 symmetry potential over a C_{2v} planar C_5 ring transition state, indicating a 3.7(1) kcal/mol barrier height and a highly puckered equilibrium geometry. Of equal importance, the double minimum potential predicts the presence of symmetric/antisymmetric pairs of tunneling states, which can be calculated in a 1D Hamiltonian with the effective mass as a function of the puckering coordinate. The predicted tunneling splittings for this puckering potential are < 1 MHz and are not resolvable in the slit jet expansion geometry. However, the results offer predictions for detection of cyclopentyl via pure rotational microwave spectroscopy, which would likely resolve such splittings and offer additional insights into the time scales and barrier heights for the tunneling of cyclopentyl radical between one well and the other.

Finally, the existence of high-resolution, assignable rovibrational spectra for such a large polyatomic at CH stretch fundamental levels of excitation is remarkable and contains valuable information on vibrational dynamics in the upper state. To help interpret such dynamics, we present an analysis and assessment for the impact of intramolecular vibrational relaxation (IVR) on such high-resolution spectra, which for the cyclopentyl radical spectra we can quantitatively deconstruct into density of states ($\rho \approx 40\text{--}90 \text{ \#/cm}^{-1}$) and coupling matrix element ($\langle H_{ij} \rangle = 0.003(1) \text{ cm}^{-1}$) contributions. Although further experimental and theoretical work will be necessary, the present high-resolution spectroscopic results suggest that the effective absence of IVR effects in the cyclopentyl radical spectra is largely due to topological constraints for the cycloalkyl ring, which eliminate the lowest frequency torsional modes present for an open linear hydrocarbon chain and which completely dominate the density of vibrational states. It will be interesting to explore further such a transition from discrete, rotationally assignable, high-resolution spectra of small molecules to the inevitable limit of near continuous absorption for larger molecules with increase in vibrational state density and bright–dark state coupling.

SUPPLEMENTARY MATERIAL

Further detailed output from the high level CCSD(T) *ab initio* calculations and predicted tunneling splittings can be found in the [supplementary material](#).

ACKNOWLEDGMENTS

This work was supported by grants from the Department of Energy (Grant No. DE-FG02-09ER16021), with initial funds for construction of the slit jet laser spectrometer provided by the National Science Foundation (Grant Nos. CHE-1665271/2053117 and PHY 1734006). D.J.N. also would like to thank John F. Stanton, T. Lam Nguyen, and P. Bryan Changala for their generous help and

patience in implementing CFOUR and large amplitude quantum software packages.

AUTHOR DECLARATIONS

Conflict of Interest

The authors have no conflicts to disclose.

Author Contributions

Andrew Kortyna: Data curation (equal); Formal analysis (equal); Writing – original draft (equal). **Melanie A. R. Reber:** Data curation (equal); Writing – review & editing (equal). **David J. Nesbitt:** Conceptualization (lead); Data curation (equal); Formal analysis (equal); Project administration (lead); Supervision (lead); Writing – original draft (equal); Writing – review & editing (equal).

DATA AVAILABILITY

The data that support the findings of this study are available within the article and its [supplementary material](#) or from the corresponding author upon reasonable request.

REFERENCES

- ¹A. McIlroy and D. J. Nesbitt, “Vibrational mode mixing in terminal acetylenes: High-resolution infrared laser study of isolated J states,” *J. Chem. Phys.* **92**, 2229 (1990).
- ²A. McIlroy and D. J. Nesbitt, “High-resolution, slit jet infrared-spectroscopy of hydrocarbons: Quantum state specific mode mixing in CH stretch-excited propyne,” *J. Chem. Phys.* **91**, 104 (1989).
- ³A. McIlroy, D. J. Nesbitt, E. R. T. Kerstel *et al.*, “Sub-Doppler, infrared-laser spectroscopy of the propyne $2\nu_1$ band: Evidence of z -axis Coriolis dominated intramolecular state mixing in the acetylenic CH stretch overtone,” *J. Chem. Phys.* **100**, 2596 (1994).
- ⁴J. Go and D. S. Perry, “Random matrix treatment of intramolecular vibrational redistribution. II. Coriolis interactions in 1-butyne and ethanol,” *J. Chem. Phys.* **103**, 5194 (1995).
- ⁵D. S. Perry, “Random matrix treatment of intramolecular vibrational redistribution. I. Methodology and anharmonic interactions in 1-butyne,” *J. Chem. Phys.* **98**, 6665 (1993).
- ⁶D. S. Perry, G. A. Bethardy, and X. L. Wang, “The effect of the torsional barrier height on the acceleration of intramolecular vibrational relaxation (IVR) by molecular flexibility,” *Ber. Bunsenges. Physik. Chem.* **99**, 530 (1995).
- ⁷D. B. Moss and C. S. Parmenter, “Acceleration of intramolecular vibrational redistribution by methyl internal rotation. A chemical timing study of p -fluorotoluene and p -fluorotoluene- d_3 ,” *J. Chem. Phys.* **98**, 6897 (1993).
- ⁸D. B. Moss, C. S. Parmenter, T. A. Peterson, C. J. Pursell, and Z. Q. Zhao, paper presented at the 7th International Symposium on Ultrafast Processes in Spectroscopy, Bayreuth, Germany, 1991.
- ⁹C. S. Parmenter and B. M. Stone, “The methyl rotor as an accelerating functional group for IVR,” *J. Chem. Phys.* **84**, 4710 (1986).
- ¹⁰J. B. Hopkins, D. E. Powers, and R. E. Smalley, “Vibrational relaxation in jet-cooled alkyl benzenes,” *J. Chem. Phys.* **71**, 3886 (1979).
- ¹¹J. B. Hopkins, D. E. Powers, and R. E. Smalley, “Vibrational relaxation in jet-cooled alkyl benzenes. III. Nanosecond time evolution,” *J. Chem. Phys.* **73**, 683 (1980).
- ¹²J. B. Hopkins, D. E. Powers, and R. E. Smalley, “Erratum: Vibrational relaxation in jet-cooled alkyl benzenes [*J. Chem. Phys.* **71**, 3886 (1979)],” *J. Chem. Phys.* **72**, 2905 (1980).
- ¹³A. McIlroy and D. J. Nesbitt, “Large amplitude skeletal isomerization as a promoter of intramolecular vibrational relaxation in CH stretch excited hydrocarbons,” *J. Chem. Phys.* **101**, 3421 (1994).
- ¹⁴S. E. Stein and B. S. Rabinovitch, “On the use of exact state counting methods in RRKM rate calculations,” *Chem. Phys. Lett.* **49**, 183 (1977).
- ¹⁵G. Z. Whitten and B. S. Rabinovitch, “Accurate and facile approximation for vibrational energy-level sums,” *J. Chem. Phys.* **38**, 2466 (1963).
- ¹⁶G. T. Buckingham, C.-H. Chang, and D. J. Nesbitt, “Correction to ‘High-resolution rovibrational spectroscopy of jet-cooled phenyl radical: The ν_{19} out-of-phase symmetric CH stretch,’” *J. Phys. Chem. A* **117**, 10047 (2013).
- ¹⁷E. N. Sharp, M. A. Roberts, and D. J. Nesbitt, “Rotationally resolved infrared spectroscopy of a jet-cooled phenyl radical in the gas phase,” *Phys. Chem. Chem. Phys.* **10**, 6592 (2008).
- ¹⁸A. Kortyna, A. J. Samin, T. A. Miller, and D. J. Nesbitt, “Sub-Doppler infrared spectroscopy of resonance-stabilized hydrocarbon intermediates: ν_3/ν_4 CH stretch modes and CH_2 internal rotor dynamics of benzyl radical,” *Phys. Chem. Chem. Phys.* **19**, 29812 (2017).
- ¹⁹M. J. H. Kemper, J. M. F. Van Dijk, and H. M. Buck, “A backtracking algorithm for exact counting of internal molecular energy levels,” *Chem. Phys. Lett.* **53**, 121 (1978).
- ²⁰N. Jiayu and H. Jianyi, “Formation and distribution of heavy oil and tar sands in China,” *Mar. Pet. Geol.* **16**, 85 (1999).
- ²¹O. P. Strausz, T. W. Mojselsky, J. D. Payzant, G. A. Olah, and G. K. S. Prakash, “Upgrading of Alberta’s heavy oils by superacid-catalyzed hydrocracking,” *Energy Fuels* **13**, 558 (1999).
- ²²P. S. Thomas, R. Chhantyal-Pun, and T. A. Miller, “Observation of the $\tilde{A}-\tilde{X}$ electronic transitions of cyclopentyl and cyclohexyl peroxy radicals via cavity ringdown spectroscopy,” *J. Phys. Chem. A* **114**, 218 (2010).
- ²³O. Nielsen and T. Wallington, in *The Chemistry of Free Radicals: Peroxy Radicals*, edited by Z. B. Alfassi (Wiley, 1997).
- ²⁴M. A. Crawford, J. J. Szenté, M. M. Maricq, and J. S. Francisco, “Kinetics of the reaction between cyclopentylperoxy radicals and HO_2 ,” *J. Phys. Chem. A* **101**, 5337 (1997).
- ²⁵E. J. Ocola, L. E. Bauman, and J. Laane, “Vibrational spectra and structure of cyclopentane and its isotopomers,” *J. Phys. Chem. A* **115**, 6531 (2011).
- ²⁶J. R. Durig and D. W. Wertz, “Vibrational spectra and structure of small-ring compounds. X. Spectroscopic evidence for pseudorotation in cyclopentane,” *J. Chem. Phys.* **49**, 2118 (1968).
- ²⁷L. E. Bauman and J. Laane, “Pseudorotation of cyclopentane and its deuterated derivatives,” *J. Phys. Chem.* **92**, 1040 (1988).
- ²⁸F. A. Houle and J. L. Beauchamp, “Thermal decomposition pathways of alkyl radicals by photoelectron spectroscopy. Application to cyclopentyl and cyclohexyl radicals,” *J. Phys. Chem.* **85**, 3456 (1981).
- ²⁹J. M. Frisch, G. W. Trucks, H. B. Schlegel *et al.*, Gaussian 09, Revision B.01, Gaussian, Inc., Wallingford, CT, 2010.
- ³⁰D. A. Matthews, L. Cheng, M. E. Harding, F. Lipparini, S. Stopkowicz, T.-C. Jagau, P. G. Szalay, J. Gauss, and J. F. Stanton, “Coupled-cluster techniques for computational chemistry: The CFOUR program package,” *J. Chem. Phys.* **152**, 214108 (2020).
- ³¹S. Davis, M. Farnik, D. Uy, and D. J. Nesbitt, “Concentration modulation spectroscopy with a pulsed slit supersonic discharge expansion source,” *Chem. Phys. Lett.* **344**, 23 (2001).
- ³²NIST chemistry webbook, NIST Standard Reference Data 60, 2022.
- ³³D. Smith and P. Spanel, in *Advances in Atomic, Molecular, and Optical Physics*, edited by B. Bederson and A. Dalgarno (Academic Press Inc., 1994), Vol. 32, p. 307.
- ³⁴E. Riedle, S. H. Ashworth, J. T. Farrell, and D. J. Nesbitt, “Stabilization and precise calibration of a continuous-wave difference frequency spectrometer by use of a simple transfer cavity,” *Rev. Sci. Instrum.* **65**, 42 (1994).
- ³⁵A. S. Pine, “High-resolution methane ν_3 -band spectra using a stabilized tunable difference-frequency laser system,” *J. Opt. Soc. Am.* **66**, 97 (1976).
- ³⁶C. M. Lovejoy and D. J. Nesbitt, “Slit pulsed valve for generation of long-path-length supersonic expansions,” *Rev. Sci. Instrum.* **58**, 807 (1987).
- ³⁷C. M. Western, “PGOPHER: A program for simulating rotational, vibrational and electronic spectra,” *J. Quant. Spectrosc. Radiat. Transfer* **186**, 221 (2017).

- ³⁸C. M. Western and B. E. Billinghurst, "Automatic assignment and fitting of spectra with PGOPHER," *Phys. Chem. Chem. Phys.* **19**, 10222 (2017).
- ³⁹P. R. Bunker and P. Jensen, *Molecular Symmetry and Spectroscopy*, 2nd ed. (NRC Research Press, Ottawa, 1998).
- ⁴⁰G. Herzberg, *Molecular Spectra and Molecular Structure. II, Infrared and Raman Spectra of Polyatomic Molecules* (Van Nostrand Reinhold Co., Toronto, 1945).
- ⁴¹J. R. Barker, "Multiple-well, multiple-path unimolecular reaction systems. I. Multiwell computer program suite," *Int. J. Chem. Kinet.* **33**, 232 (2001).
- ⁴²J. R. Barker, T. L. Nguyen, J. F. Stanton *et al.*, Multiwell program suite, 2021.
- ⁴³J. T. Hougen, P. R. Bunker, and J. W. C. Johns, "The vibration-rotation problem in triatomic molecules allowing for a large-amplitude bending vibration," *J. Mol. Spectrosc.* **34**, 136 (1970).
- ⁴⁴D. J. Rush and K. B. Wiberg, "Ab initio CBS-QCI calculations of the inversion mode of ammonia," *J. Phys. Chem. A* **101**, 3143 (1997).
- ⁴⁵J. H. Baraban, M. A. Martin-Drumel, P. B. Changala *et al.*, "The molecular structure of *gauche*-1,3-butadiene: Experimental establishment of non-planarity," *Angew. Chem., Int. Ed.* **57**, 1821 (2018).
- ⁴⁶M. C. McCarthy, S. Thorwirth, C. A. Gottlieb, and P. Thaddeus, "Tetrasulfur, S₄: Rotational spectrum, interchange tunneling, and geometrical structure," *J. Chem. Phys.* **121**, 632 (2004).
- ⁴⁷J. P. Porterfield, J. H. Westerfield, L. Satterthwaite *et al.*, "Rotational characterization of the elusive *gauche*-isoprene," *J. Phys. Chem. Lett.* **10**, 1981 (2019).
- ⁴⁸W. D. Lawrance and A. E. W. Knight, "Direct deconvolution of extensively perturbed spectra: The singlet-triplet molecular eigenstate spectrum of pyrazine," *J. Phys. Chem.* **89**, 917 (1985).
- ⁴⁹W. D. Lawrance and A. E. W. Knight, "Reply to comment on 'Direct deconvolution of extensively perturbed spectra: The singlet-triplet molecular eigenstate spectrum of pyrazine,'" *J. Phys. Chem.* **95**, 7557 (1991).